

## Review Article

# Diffusion tensor imaging of normal and injured developing human brain – a technical review

J. Neil,<sup>1,2\*</sup> J. Miller,<sup>1</sup> P. Mukherjee<sup>1</sup> and P. S. Hüppi<sup>3,4</sup>

<sup>1</sup>Department of Radiology, Washington University School of Medicine, 660 South Euclid, St Louis, MO 63110, USA

<sup>2</sup>Division of Pediatric Neurology, St Louis Children's Hospital, One Children's Place, St Louis, MO 63110, USA

<sup>3</sup>Department of Pediatrics, Children's Hospital, University Hospitals of Geneva, 6 rue Willy-Donze, 1211 Geneva 14, Switzerland

<sup>4</sup>Department of Neurology, Children's Hospital, Harvard Medical School, 300 Longwood Ave, Boston, MA 02115, USA

Received 16 May 2001; Revised 22 August 2001; Accepted 5 September 2001

**ABSTRACT:** The application of diffusion tensor imaging (DTI) to the evaluation of developing brain remains an area of active investigation. This review focuses on the changes in DTI parameters which accompany both brain maturation and injury. The two primary pieces of information available from DTI studies—water apparent diffusion coefficient and diffusion anisotropy measures—change dramatically during development, reflecting underlying changes in tissue water content and cytoarchitecture. DTI parameters also change in response to brain injury. In this context, not only does DTI offer the possibility of detecting injury earlier than conventional imaging methods, but also appears more sensitive to disruption of white matter than any other imaging method. DTI offers unique insight into brain injury and maturation, and does so in a fashion that can be readily applied in a clinical setting. Copyright © 2002 John Wiley & Sons, Ltd.

**KEYWORDS:** diffusion; brain; anisotropy; newborn; development

## INTRODUCTION

The developing human brain presents several challenges for the application of diffusion tensor imaging (DTI). Values for the water apparent diffusion coefficient and diffusion anisotropy differ markedly between pediatric brain and adult brain. Further, these parameters vary with age. As a result, much of the knowledge regarding DTI derived from studies of mature, adult human brain is not directly applicable to developing brain. Yet in these challenges also lies opportunity, as changes in water apparent diffusion coefficient and diffusion anisotropy during development provide unique insight into brain maturation. For example, water diffusion anisotropy values for white matter are extraordinarily sensitive to white matter development.<sup>1–4</sup>

In addition to providing information on brain maturation,

DTI may be used to evaluate brain injury. It is well known from studies of animals<sup>5</sup> and adult humans<sup>6</sup> that DTI excels as an early indicator of stroke, often demonstrating image abnormalities on water diffusion maps well before CT or conventional MRI.<sup>7</sup> Early detection of injury is particularly critical in the context of administration of neuroprotective agents to infants. These agents must typically be administered quickly, within hours of onset of injury, in order to interrupt the cascade of irreversible brain injury. Because these interventions are in themselves not without risk to the developing brain, it is of utmost importance to develop imaging tools that can reliably identify ongoing brain injury early to prevent treatment of non-injured patients.<sup>8</sup> Water diffusion maps derived from DTI may provide the means for this early detection of injury. DTI may also serve as a method for monitoring neuroprotective therapy by providing information on the extent of lesion development or reduction during and immediately after the administration of these agents. Finally, changes in diffusion characteristics provide early evidence of both focal and diffuse brain injury in association with periventricular leukomalacia (PVL), the most common form of white matter injury in the preterm infant.<sup>9</sup> Thus, DTI has terrific potential for assessing brain injury and therapeutic response, although it is important to bear in

\*Correspondence to: J. Neil, Department of Radiology, Washington University, School of Medicine, 660 South Euclid, St Louis, MO 63110, USA.

Contract/grant sponsor: NIH; contract grant number: NS37357.

Contract/grant sponsor: Swiss National Foundation; contract grant number: 32-56927.99.

Contract/grant sponsor: Sigrist Foundation of the University of Berne.

**Abbreviations used:** DTI, diffusion tensor imaging; PVL, periventricular leukomalacia.

mind that correlations between abnormalities on DTI and ultimate neurologic/cognitive outcome have not yet been fully determined for newborns.

In the review to follow, we will discuss the changes in DTI parameters associated with normal brain maturation as well as their response to brain injury. It is worth noting that the precise DTI parameters to employ are open to question. There is a general consensus that the directionally averaged, rotationally invariant water diffusion coefficient (the average apparent diffusion coefficient, or  $D_{av}$ ) is a useful parameter to derive from the diffusion tensor and serves as an indicator of brain maturation and/or injury. This is typically computed as one-third the trace of the diffusion tensor.<sup>10,11</sup> In contrast, the descriptions of water diffusion anisotropy used by different research groups varies (e.g. lattice anisotropy index, relative anisotropy, fractional anisotropy,  $A_{\sigma}$ , color directional plots of anisotropy, 'vector maps' or 'whisker plots', gamma variate anisotropy images). These different representations of anisotropy are related to one another; their mathematical inter-conversions ranging from multiplication by a simple constant to complete recalculation using the underlying eigenvectors.<sup>12</sup> Further, the optimal means by which to display water diffusion anisotropy remains an area of active investigation.<sup>13</sup> For more detailed information on this topic, the reader is referred to the technically oriented diffusion anisotropy article in this volume of *NMR in Biomedicine*.<sup>14</sup> In the discussion to follow, we will use the parameters,  $D_{av}$ , relative anisotropy (RA) and vector maps. Note that  $D_{av}$  is calculated as one-third of the trace of the diffusion tensor, and provides the overall magnitude of water diffusion independent of anisotropy. RA is an indicator of the degree of water diffusion anisotropy independent of the overall water diffusion coefficient. RA is zero for isotropic diffusion (diffusion that is equal in all directions) and approaches 2 as anisotropy increases. Notably, RA is linear over the total range of anisotropy values.<sup>12</sup> Vector maps, which are typically overlaid on structural images, indicate the orientation of the major eigenvector of the diffusion tensor. They provide an indication of the direction in which water diffusion is highest, which typically is parallel to white matter tracts. All three parameters are orientation-independent, meaning that they are not affected by the position of the subject in the MR scanner magnet relative to the orientation of the magnetic field gradients used to measure the diffusion values.

One aspect of DTI which differs between newborn infants and adults is the optimum  $b$  value at which to make the measurement. In general, a  $b$  value corresponding to approximately  $1.1/D_{av}$  provides the greatest contrast-to-noise ratio for such a measurement.<sup>15</sup> In adult humans, the high  $b$  value is typically on the order of  $1000 \text{ mm}^2 \text{ s}^{-1}$ . For infant brain, which has higher values for  $D_{av}$ ,  $b$  values on the order of  $700\text{--}800 \text{ mm}^2 \text{ s}^{-1}$  are used. Otherwise, similar MR pulse sequences and post

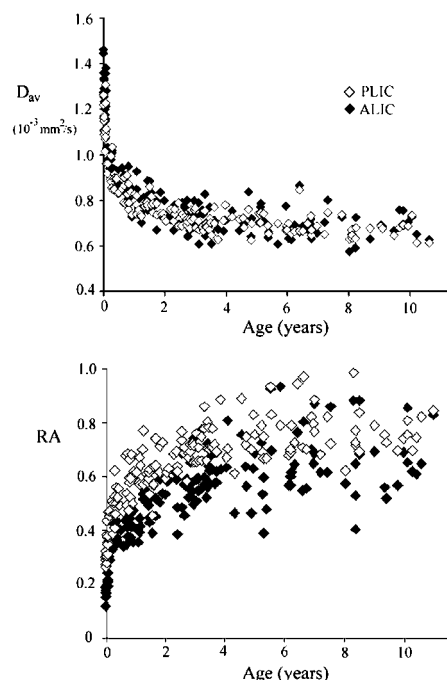


**Figure 1.** Plots of the changes in  $D_{av}$  and RA of the anterior and posterior limbs of the internal capsule vs age. The data start at 26 weeks gestational age with zero taken as 40 weeks gestational age. There are a total of 166 data points. Data are included from Neil *et al.*<sup>3</sup> and Mukherjee *et al.*<sup>16</sup> The values for  $D_{av}$  are somewhat higher in the anterior limb of the internal capsule than the posterior limb early in life, but by a few months of age the values are identical<sup>16</sup> at approximately  $0.69 \times 10^{-3} \text{ mm}^2 \text{ s}^{-1}$ . The values for RA, on the other hand, tend to be higher in the posterior limb of the internal capsule than for the anterior limb throughout life, with the difference becoming smaller with increasing age. The asymptotic RA values for the anterior and posterior limbs of the internal capsule are 0.66 and 0.78, respectively, though the true values may be somewhat lower because of noise bias in the data.<sup>16</sup>

processing methods are used for both infant and adult human brain DTI.

## DTI IN NORMAL BRAIN DEVELOPMENT

$D_{av}$  values differ between pediatric and adult human brain in two primary ways. First,  $D_{av}$  values are higher for pediatric brain than adult. For example,  $D_{av}$  values for the white matter of the centrum semiovale in premature infants<sup>2,3</sup> approach  $2.0 \times 10^{-3} \text{ mm}^2 \text{ s}^{-1}$ , while values for adult brain are typically  $0.7 \times 10^{-3} \text{ mm}^2 \text{ s}^{-1}$ . As shown in Fig. 1,  $D_{av}$  values decrease with increasing age in a monotonic fashion during development until they reach adult values.<sup>16–21</sup> Second,  $D_{av}$  maps of pediatric brain show contrast between white and gray matter, with the  $D_{av}$  values for white matter being higher than those for gray (Fig. 2). Note that the  $D_{av}$  maps show strong contrast in the image from the 26-week premature infant. This

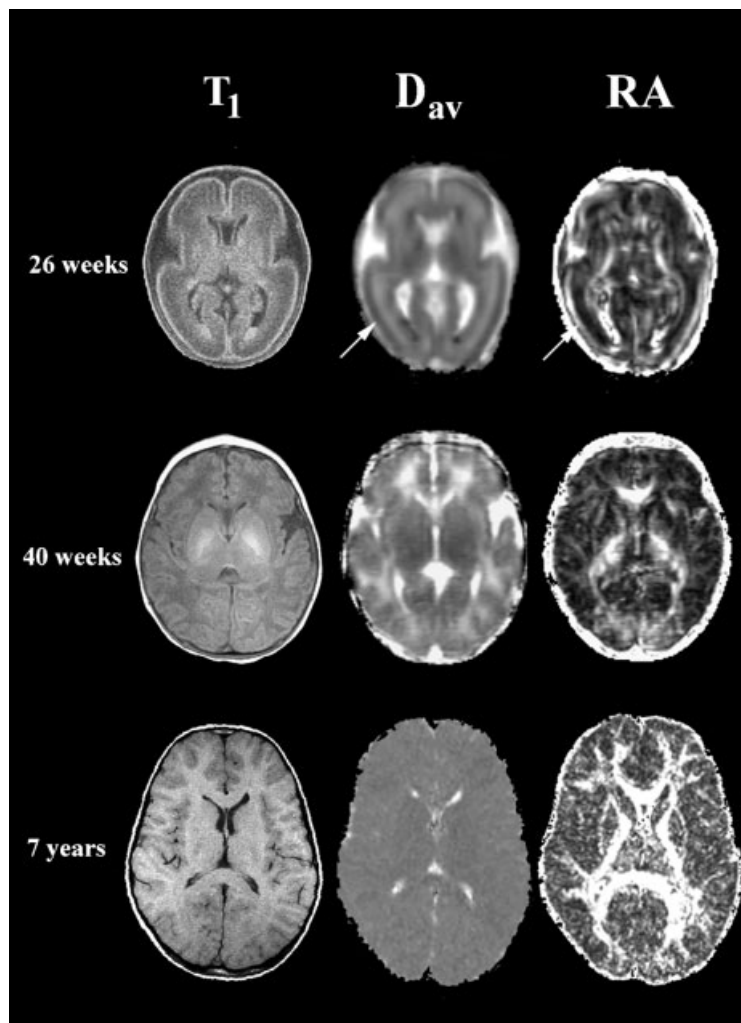


**Figure 2.** Axial images at the level of the basal ganglia from subjects of differing ages. Anterior is up and posterior is down. The top row is from a premature infant of 26 weeks gestational age. The middle row is from a term infant of 40 weeks gestational age. The bottom row is from a 7-year-old. The left column consists of  $T_1$ -weighted images for anatomic reference. The center column consists of  $D_{av}$  parametric maps for which higher values of  $D_{av}$  appear brighter. The right column consists of RA parametric maps for which higher values of RA appear brighter. All three subjects were normal at the time of the study. The images are not shown exactly to size scale (the head size of the premature infant is considerably smaller than that of the 7-year-old). There is a small amount of blood in the occipital horns of the lateral ventricles from the 26-week infant, representing an intraventricular hemorrhage. Note the increase in cortical folding which accompanies development, with the premature brain appearing lissencephalic in comparison with the mature brains. Note also that there is strong gray–white contrast on the  $D_{av}$  maps from the premature infant. This contrast is diminished at 40 weeks and no longer present by age 7 years. The RA map from the premature infant shows RA values above background for the anterior and posterior limbs of the internal capsule, but is especially notable for RA values above background in the developing cerebral cortex (arrows). This relatively high cortical anisotropy disappears by 40 weeks gestation. At 40 weeks, RA values are significantly higher for the myelinated posterior limb of the internal capsule as compared with the unmyelinated anterior limb.<sup>3</sup> In the progression from 26 weeks gestation to 7 years, white matter RA values increase first in the occipital lobe (at 40 weeks) but by age 7 years are increased relatively uniformly throughout the subcortical white matter. A portion of this figure is reproduced by permission of RSNA Publications.<sup>3</sup>

contrast is already diminishing by term (40 weeks) and has vanished by age 7 years. This contrast does not return with further increases in age.  $D_{av}$  maps of adult brain show essentially equal  $D_{av}$  values for white and gray matter<sup>22</sup> when measured with  $b$  values  $\leq 1000 \text{ s mm}^{-2}$ . As can be seen in Figs 1 and 2, changes in  $D_{av}$  take place much more rapidly in early development, especially during the first year of life. These changes are not necessarily simultaneous in all brain regions. They take place earlier, for example, in the posterior limb of the internal capsule than the anterior limb.<sup>2,3</sup> This may be related to the fact that the posterior limb myelinates earlier.

The precise cause of the decrease in  $D_{av}$  with increasing age is not known, although it has been postulated that the rapid decrease observed between early gestation and term is due to the concomitant decrease in overall water content.<sup>3</sup> For reference, the  $D_{av}$  of free water at body temperature is approximately  $3.0 \times 10^{-3} \text{ mm}^2 \text{ s}^{-1}$ . Thus, there is some restriction to water motion even for the highest  $D_{av}$  values measured in premature infants, which are on the order of  $2.0 \times 10^{-3} \text{ mm}^2 \text{ s}^{-1}$ . Brain water content decreases dramatically with increasing gestational age.<sup>23</sup> As it does, structures that hinder water motion (e.g. cell and axonal membranes) become more densely packed, increasing restriction to motion; as if the brain becomes more viscous as its water content decreases. Differences in water content may also underlie the contrast present between white and gray matter in pediatric brain, although not in a simple fashion. In adult brain, the water content of white matter is substantially lower than that of gray matter (65 vs 85%<sup>23</sup>), yet the  $D_{av}$  values for the two regions are virtually identical.<sup>22</sup> This implies that white matter is less restrictive to water motion than gray matter at a given water content. This may be related to the fact that water motion parallel to axons is relatively unrestricted, especially in comparison to motion perpendicular to axons or in gray matter. In the premature brain, water content is similar in white and gray matter.<sup>23</sup> The finding of higher  $D_{av}$  values in white matter than gray for premature brain despite their similar water content is also consistent with the idea that white matter is less restrictive to water motion than gray matter. In adult brain, this difference in restriction appears to be offset by the differing water contents of the two areas.

RA values also differ between adult and pediatric brain. For children beyond term and for adults, RA values for cortical gray matter are consistent with zero, meaning that water diffusion in gray matter is isotropic at the spatial resolutions currently available. RA values for white matter areas, on the other hand, are relatively low in infants and increase steadily with increasing age<sup>24</sup> (Fig. 1). As with changes in values for  $D_{av}$ , changes in RA take place more quickly early in development. While changes in  $D_{av}$  and RA for white matter typically take place in tandem, with  $D_{av}$  values decreasing and RA

values increasing during maturation, it is important to bear in mind that the two parameters are theoretically independent of one another. Thus, a change in one is not always accompanied by the opposite change in the other. For example, the decrease of RA of cerebral cortex that takes place between 26 and 32 weeks gestational age is accompanied by a decrease in  $D_{av}$ .<sup>25,26</sup>

The increase in white matter RA values during development appears to take place in two steps. The first increase takes place *before* the histologic appearance of myelin.<sup>1-3</sup> This increase has been attributed to changes in white matter structure which accompany the 'pre-myelinating state'.<sup>1</sup> This state is characterized by a number of histologic changes, including an increase in the number of microtubule-associated proteins in axons, a change in axon caliber, and a significant increase in the number of oligodendrocytes. It is also associated with changes in the axonal membrane, such as an increase in conduction velocity and changes in  $\text{Na}^+/\text{K}^+$ -ATPase activity. It is not yet clear how these changes lead to an increase in RA. The second, more sustained increase in RA, is associated with the histologic appearance of myelin and its maturation. The increase in anisotropy associated with premyelination is notable in that it takes place in the absence of changes in  $T_1$ - or  $T_2$ -weighted imaging as well as before the histologic appearance of myelin.<sup>3</sup> Thus, it constitutes the earliest indication of impending myelination. This two-stage increase in white matter anisotropy takes place at different rates for different brain areas, as does myelination.<sup>27</sup> For example, RA changes take place earlier in the white matter underlying visual cortex than other subcortical white matter. As can be seen in Fig. 2, RA values are relatively low in occipital white matter for the 26 week infant but are clearly increasing at 40 weeks, with values on the order of 0.17 at term (unpublished data). Thus, increases in RA may serve as an indicator of systems which are coming 'on line'.

While myelination accounts for much of the increase in RA associated with brain maturation, it is not the whole story. Diffusion anisotropy will be present under any circumstance in which the cytoarchitecture of the tissue is arranged in such a way as to lead to greater hindrance of water motion in one direction as compared with others. For example, the anterior limb of the internal capsule contains regularly arranged unmyelinated axons which, despite the absence of myelin, are arranged in such a way as to lead to diffusion anisotropy. This can be seen in the RA map from the 26 week infant in Fig. 2. It is instructive to compare the RA maps of the anterior and posterior limbs of the internal capsule at term. As can be seen in the RA map at 40 weeks gestation, the posterior limb has considerably higher RA than the anterior limb, and values for the anterior limb at term are 0.18, as compared with 0.30 for the posterior limb.<sup>3</sup> While both anterior and posterior limbs probably have similar axonal organization, the posterior limb is myelinated at birth

while the anterior limb is not. As a result, the higher RA of the posterior limb is likely to be, at least in part, due to the presence of myelin. However, in older children, when both areas are fully myelinated, the anterior limb still has lower RA values than the posterior limb; 0.66 vs 0.78.<sup>16</sup> Thus the RA values of the posterior limb are 66% higher than the anterior limb at birth, when the posterior limb is myelinated and the anterior limb is not, and 18% higher in young adults, when both areas are myelinated. This suggests that approximately half the anisotropy found in this particular white matter system can be ascribed to the presence of myelin, though this is clearly an oversimplification, as anisotropy can be influenced by other factors such as axon packing, relative membrane permeability to water, internal axonal structure, and tissue water content. While the present discussion is focused on data from newborn infants, there is long-standing precedent for water diffusion anisotropy in axon bundles in the absence of myelin from both animal and human studies. There have also been other estimates of the relative contribution of myelin to anisotropy. These topics are reviewed in detail in this volume of *NMR in Biomedicine*.<sup>28</sup>

Another brain area in which RA values differ between pediatric and adult brain is cerebral cortex. RA values of cortical grey matter in adult brain are generally consistent with zero (i.e. diffusion is isotropic). As shown in Fig. 2, RA values for cortical gray matter in premature brain are transiently nonzero during development.<sup>25,26</sup> A similar phenomenon has been observed for kitten,<sup>29</sup> piglet,<sup>30</sup> and mouse.<sup>31</sup> In humans, the values are nonzero for the earliest gestational ages studied (26 weeks in Fig. 2) and decrease to near zero by 32 weeks.<sup>25</sup> The transient presence of anisotropy has been attributed to cortical cytoarchitecture. During the gestational ages for which anisotropy values are nonzero, cortical cytoarchitecture is dominated by the radial glial fibers that are present across the cortical strata and by the radially oriented apical dendrites of pyramidal cells.<sup>32</sup> With time, this architecture is disrupted by the addition of basal dendrites as well as thalamocortical afferents, which tend to be oriented orthogonal to the apical dendrites. Thus developmental changes in RA of cerebral cortex reflect changes in its microstructure.

Vector maps also provide information regarding anisotropy. In the case of cortical gray matter, the vectors are oriented radially, consistent with the orientation of the radial glial fibers and apical dendrites of pyramidal cells.<sup>25</sup> As shown in Fig. 3, vector maps of white matter provide a visual indication of white matter organization. Thus it is possible to produce an image of the overall orientation of white matter fibers in a given area. Alteration of white matter organization in preterm infants compared with fullterm newborns has been shown using DTI.<sup>2</sup> As discussed below, this orientation may be disrupted due to injury. It is also worth noting that vector maps can be used to follow white matter tracts as they

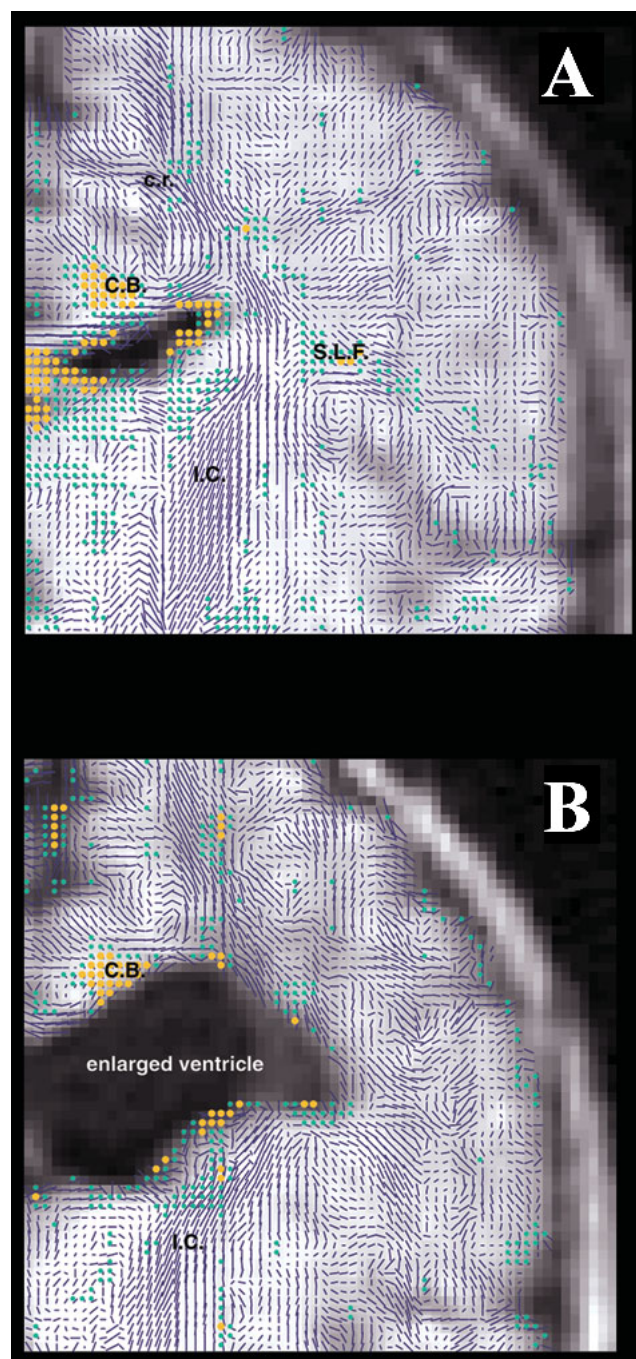


**Figure 3.** Diffusion vector maps overlaid on coronal diffusion-weighted images for a premature infant at term with no white matter injury (A) and a premature infant at term with perinatal white matter injury (B). The posterior limb of the internal capsule (I.C.) in (A) shows more homologous directed vectors that are longer and more densely packed than in the internal capsule of (B). Anteroposterior-oriented white matter fibers in the area of the superior longitudinal fasciculus (SLF; yellow and green dots with yellow representing higher RA than green) in (A) indicate the presence of fiber bundles that are missing or are less prominent in (B). The only discrete anteroposterior fiber bundles that definitely are present in (B) are the cingulate bundle (C.B.). Fibers of the corona radiata (c.r.) appear less well-organized in (B) than (A). Reproduced with permission from *Pediatrics*, Vol. 107, Page(s) 459, Figure 3, Copyright 2001.<sup>73</sup>



course through the brain.<sup>33</sup> While this method has been applied to adult humans and animals, it has yet to be applied to infants. This may be related to the fact that the task of tract tracing is made more difficult in infants by the lower values for RA (and hence decreased contrast-to-noise ratio). Further, tract tracing studies typically require higher spatial resolution than conventional DTI. This engenders longer scan times, which are less acceptable for younger subjects. However, it is likely that such studies will be applied to infants and children in the future, especially for areas of white matter that have myelinated by the time the subject is studied. As of yet, however, the necessary normative data on vector maps of neonatal brain have not been published.

## DTI AND INJURY DURING BRAIN DEVELOPMENT

A comprehensive discussion linking the pathophysiology of newborn brain injury with changes in DTI parameters is not yet possible at our current level of understanding. The existence of the many hypotheses outlined below to explain brain injury in newborns is a testament to both its complexity and the fact that it is not yet fully understood. Further, the cause(s) of the decrease in water  $D_{av}$  associated with brain injury remains an area of active debate. Nevertheless, we will review this literature briefly. For a more comprehensive review on neonatal brain injury, the reader is referred to Volpe.<sup>34</sup>

Whereas adult stroke is typically a thromboembolic event in which reperfusion may or may not occur, neonatal brain injury is characterized by hypoperfusion and/or hypoxemia followed by reperfusion as the infant is resuscitated, typically shortly after delivery. Hypotheses put forth to explain brain injury often take both mechanisms, hypoxia/ischemia and reperfusion, into account. Neuronal death appears to involve both necrosis and apoptosis.<sup>35</sup> Molecular mechanisms proposed to explain injury to both neurons and glia include accumulation of: cytosolic calcium,<sup>36</sup> free radicals (including nitric oxide),<sup>37</sup> cytotoxic amino acids,<sup>38</sup> and cytokines.<sup>39,40</sup> Periventricular leukomalacia, PVL, is a unique pattern of neonatal brain injury that is most often found in preterm infants. Pathologic abnormalities are characteristically localized to the white matter dorsal and lateral to the external angles of the lateral ventricles and involve primarily the centrum semiovale.<sup>41</sup> This white matter region is thought especially vulnerable to injury in the preterm infant because of the nature of its blood supply<sup>42</sup> and particular sensitivity to proinflammatory cytokines triggered by stimuli such as hypoxia-ischemia and infection.<sup>43–45</sup> Recently a role for low arterial partial pressure of carbon dioxide has been postulated as well.<sup>46</sup>

As indicated in the introduction, values for  $D_{av}$  decrease quickly after injury in most models studied, providing evidence of injury on maps of  $D_{av}$  before the

injury is detectable on conventional imaging. (Note that a decrease in  $D_{av}$  appears dark on  $D_{av}$  maps but bright on 'diffusion-weighted' images.) The decrease in water diffusion associated with injury was initially described for animal<sup>5,47</sup> and adult human<sup>6</sup> stroke, and was subsequently confirmed for human infants.<sup>48</sup> There is not yet a consensus on the precise mechanism for the decrease in  $D_{av}$  associated with injury. The most commonly cited hypothesis invokes a two-compartment (intracellular and extracellular) model for brain water. This explanation rests on two basic assumptions: (1) there is a shift of water from the extra- to intracellular space in association with injury; and (2) water in the extracellular space has a 'faster' or higher diffusion coefficient than water in the intracellular space. If these conditions are met, and the overall water diffusion detected by DTI is a weighted average of the diffusion coefficients of water in the two compartments, then the shift of water from the 'faster-diffusing' extracellular compartment to the 'slower-diffusing' intracellular compartment could explain the overall decrease in  $D_{av}$  which accompanies brain injury.<sup>5</sup> It is worth noting that the second assumption above, that of different diffusion coefficients for water in the two compartments, has not been confirmed. However, there are marker data which indicate that water diffusion is similar in the two compartments.<sup>49</sup> Further, several labs have noted a marked decrease in the diffusion of intracellular markers with brain injury.<sup>50–52</sup> Thus, there is evidence that the decrease in  $D_{av}$  associated with brain injury is driven by a decrease in the diffusion coefficient of intracellular water, which comprises more than 80% of total brain water.

It should be noted that there are clinical circumstances under which  $D_{av}$  increases rather than decreases immediately after injury. In general, it appears that  $D_{av}$  values decrease under conditions of cell injury and cytotoxic edema, but increase under conditions of vasogenic edema.<sup>53</sup> One well-studied example is reversible posterior leukoencephalopathy syndrome. This condition is not found in newborns, and typically occurs in response to immunosuppressive therapy or hypertension.<sup>54</sup> The underlying pathophysiology appears to be damage to the vascular endothelium leading to vasogenic (rather than cytotoxic) edema. The vasogenic edema is characterized by an increase in local brain water content without direct cell injury. This increase in water content appears to bring about an increase in  $D_{av}$ .<sup>55,56</sup> Another pathologic condition in which  $D_{av}$  may increase is high-pressure hydrocephalus. An increase in  $D_{av}$  has been reported for animal models<sup>53,57</sup> as well as adult humans.<sup>58</sup> In a study of newborn infants with posthemorrhagic hydrocephalus, Hüppi *et al.* noted a marked increase in  $D_{av}$  values in areas adjacent to dilated cerebral ventricles. These changes were associated with a more widespread reduction in white matter RA values. They note that these findings could be related to transependy-

mal migration of CSF into the interstitial space, long-term sequelae of injury to periventricular white matter, or some combination of both mechanisms.<sup>59</sup>

Changes in  $D_{av}$  following injury are dynamic.  $D_{av}$  values are initially decreased, but subsequently increase so that they are greater than normal and remain so in the chronic phase of injury. During the transition between decreased and increased values there is a brief period during which values are normal, a process referred to as 'pseudonormalization'. Pseudonormalization takes place roughly two days following stroke in a rat model<sup>60,61</sup> and at approximately 9 days following injury in adult human stroke.<sup>62</sup> Preliminary data indicate that the timing of pseudonormalization in human newborns more closely follows that of adult humans than rodents, taking place at roughly seven days following the injury.<sup>26</sup> The time course of these changes is complex, however, and may vary somewhat with the nature of the injury (hypoxia-ischemia, inflammation, trauma), the relative vulnerability of different brain areas to injury, and other processes such as primary and secondary energy failure.<sup>61</sup> Given the dynamic nature of these changes, it has been suggested that a combination of conventional and DTI images can be used to estimate the age of an injury to the central nervous system.<sup>60</sup> During the first days following an injury, there are abnormalities on  $D_{av}$  maps, due to decreased water  $D_{av}$ , but not  $T_2$ -weighted images. Subsequently, abnormalities are visible on both  $D_{av}$  maps and  $T_2$ -weighted images. Roughly one week after the injury, the  $D_{av}$  map will become normal due to pseudonormalization, but the injury will be visible on  $T_2$ -weighted images. With chronic injury, the lesion will be visible again on  $D_{av}$  maps, but now as an increase in water  $D_{av}$  rather than a decrease.

The dynamic nature of the changes in  $D_{av}$  following injury makes it difficult to directly compare conventional MRI with DTI for detection of injury. Which method is most sensitive to injury— $T_2$ -weighted imaging,  $T_1$ -weighted imaging or  $D_{av}$  maps—varies with time after injury. Studies in which MR imaging is done at roughly one week after injury, the approximate time at which pseudonormalization takes place, tend to find that conventional imaging is as good as or better than DTI.<sup>63</sup> Studies in which the imaging is done somewhat earlier<sup>64,65</sup> tend to find more utility for DTI. Studies in which a series of images are obtained from the same infant over time<sup>26</sup> indicate that DTI is more useful during the first few days after injury, whereas conventional imaging, particularly  $T_2$ -weighted or FLAIR imaging, is more useful at later times. Overall, the primary difference between DTI and conventional imaging is the capability of DTI to often detect injury earlier. This may offer advantages in the future if neuroprotective agents become available and early detection of injury becomes important for deciding whether or not to administer them to a particular patient. It is worth noting, however, that DTI may not necessarily always demonstrate injury earlier

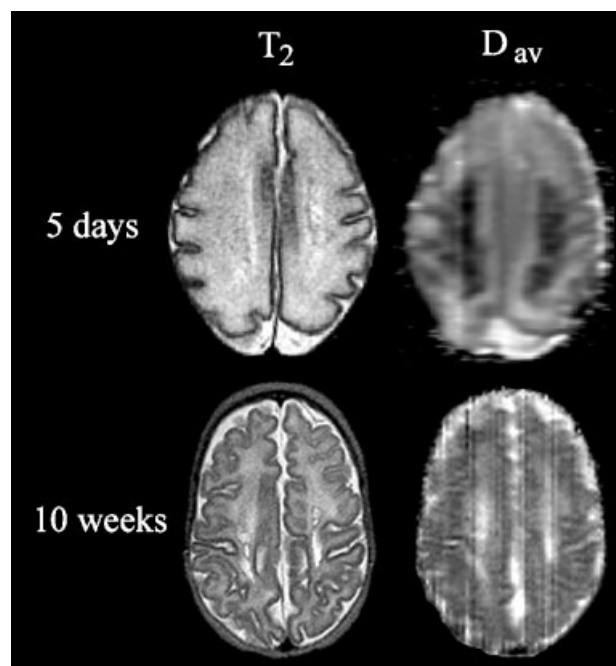


**Figure 4.** Axial images at the level of the centrum semiovale from an infant of 30 weeks gestation with periventricular leukomalacia (PVL). The notations above the images indicate the image type; those on the left indicate the age of the infant at the time of the imaging study. The  $T_2$ -weighted image from 5 days of age shows subtle areas of increased signal in the periventricular white matter. The corresponding  $D_{av}$  map shows much more widespread and distinct areas of reduced diffusion, visible as dark areas, in the periventricular region. At age 10 weeks, periventricular white matter injury with cystic change is visible on the  $T_2$ -weighted image. The  $D_{av}$  map at this age shows corresponding areas of increased diffusion, consistent with maturation of the white matter injury. This case indicates that DTI may show brain injury earlier than conventional MR imaging.<sup>64</sup> Reproduced by permission of Mosby Publishing Inc.

than conventional MR imaging. Highly detailed animal studies indicate that, under conditions of milder injury, the decrease in  $D_{av}$  may be delayed, not necessarily showing the injury earlier than conventional MR.<sup>61,66</sup> While this has yet to be described for human newborns, it remains possible that a fraction of injury may not be evident on early  $D_{av}$  maps, corresponding to the 'diffusion-negative stroke' described for adult humans.<sup>67</sup>

There is evidence that  $D_{av}$  maps not only may show injury earlier than conventional MR imaging (Fig. 4), but also show injury that is not detectable by other imaging methods. One notable example from newborns is the acute stage of PVL, which is readily detectable as a decrease in signal on  $D_{av}$  maps but is often not detectable on conventional imaging until at least 3 days after injury.<sup>64,68</sup> In addition, widespread abnormalities in  $D_{av}$  are detectable in some newborns suffering from hypoxic-ischemic injury in the absence of corresponding abnormalities on conventional MR imaging.<sup>65</sup>

RA of white matter also changes following injury. The changes appear to take place over several days to weeks, though detailed time course studies are not yet available. At the simplest level, RA values are reduced dramatically in areas in which white matter is lost, such as porencephalic cysts.<sup>69</sup> At a more complex level, RA values of white matter connecting Wernicke's area with Broca's area in adult brain appear to correlate strongly with reading ability.<sup>70</sup> Studies on adults with stroke also indicate that Wallerian degeneration is detectable as changes in RA distant from the site of infarction in adults.<sup>71</sup> Changes in anisotropy involving both RA and vector maps will likely prove especially relevant in premature infants, who tend to sustain injury to white matter.<sup>72</sup> In the chronic stage of PVL, reductions in RA may be present and vector maps may show disruption of white matter tracts distant from the focal, cystic lesions detected by conventional imaging (Fig. 3). In this case, changes in RA are detectable not only near the site of primary injury (the periventricular white matter), but also in the posterior limb of the internal capsule, indicating a disturbance of developing fibers which project through this area.<sup>73</sup> Thus, RA and vector maps demonstrate injury that is not detectable by more conventional means. Further, changes in RA and fiber maps may provide insight into postinjury brain plasticity. The clinical relevance of injury and related modification of white matter architecture detected in this fashion is not yet known, and long-term follow up studies are currently underway.

## CONCLUSIONS

Striking changes in water apparent diffusion coefficient and diffusion anisotropy accompany brain maturation. The changes in water apparent diffusion are likely related to changes in brain water content. Changes in anisotropy, on the other hand, are apparently linked to changes in tissue microstructure. In the case of grey matter, this may reflect changes in the dendritic architecture of pyramidal cells. In the case of white matter, this is due to both 'premyelination' changes and myelination itself. Thus DTI offers a unique, noninvasive window into brain maturation which can be readily applied to human development.

DTI parameters also show distinct changes in response to brain injury. Decreases in the water apparent diffusion coefficient may serve as an early indicator of brain injury which could prove useful in the context of rapidly determining the presence/absence of injury in anticipation of therapeutic intervention with neuroprotective agents for the developing brain. Changes in water anisotropy are extraordinarily sensitive to injury-related impairment of subsequent white matter development, providing evidence of disruption in areas much more widespread than detected through conventional imaging.

Thus DTI is potentially of great value clinically for evaluation of injury and plasticity in developing brain.

## Acknowledgements

Supported by NIH grant NS37357 (JJN and JM), the Swiss National Foundation 32-56927.99 (PSH) and the Sigrist Foundation of the University of Berne (PSH).

## REFERENCES

1. Wimberger DM, Roberts TP, Barkovich AJ, Prayer LM, Moseley ME, Kucharczyk J. Identification of "premyelination" by diffusion-weighted MRI. *J. Comput. Assist. Tomogr.* 1995; **19**: 28–33.
2. Huppi PS, Maier SE, Peled S, Zientara GP, Barnes PD, Jolesz FA, Volpe JJ. Microstructural development of human newborn cerebral white matter assessed *in vivo* by diffusion tensor magnetic resonance imaging. *Pediatr. Res.* 1998; **44**: 584–590.
3. Neil JJ, Shiran SI, McKinstry RC, Scheff GL, Snyder AZ, Almli CR, Akbudak E, Aaronovitz JA, Miller JP, Lee BCP, Conturo TE. Normal brain in human newborns: Apparent diffusion coefficient and diffusion anisotropy measured using diffusion tensor imaging. *Radiology* 1998; **209**: 57–66.
4. Huppi PS. MR imaging and spectroscopy of brain development. *Magn. Reson. Imag. Clin. N. Am.* 2001; **6**: 1–18.
5. Moseley ME, Cohen Y, Mintorovitch J, Chileuitt L, Shimizu H, Kucharczyk J, Wendland MF, Weinstein PR. Early detection of regional cerebral ischemia in cats: comparison of diffusion- and T<sub>2</sub>-weighted MRI and spectroscopy. *Magn. Reson. Med.* 1990; **14**: 330–346.
6. Warach S, Chien D, Li W, Ronthal M. Fast magnetic resonance diffusion-weighted imaging of acute human stroke. *Neurology* 1992; **42**: 1717–1723.
7. Bryan RN, Levy LC, Whitlow WD, Killian JM, Prezios TJ, Rosario JA. Diagnosis of acute cerebral infarction: Comparison of CT and MR imaging. *Am. J. Neuroradiol.* 1990; **12**: 611–620.
8. Nelson KB, Leviton A. How much of neonatal encephalopathy is due to birth asphyxia? *Am. J. Dis. Child.* 1991; **145**: 1325–1331.
9. Inder TE, Huppi PS, Warfield S, Kikinis R, Zientara GP, Barnes PD, Jolesz F, Volpe JJ. Periventricular white matter injury in the premature infant is followed by reduced cerebral cortical gray matter volume at term. *Ann. Neurol.* 1999; **46**: 755–760.
10. Decanniere C, Eleff S, Davis D, van Zijl PCM. Correlation of rapid changes in the average water diffusion constant and the concentrations of lactate and ATP breakdown products during global ischemia in cat brain. *Magn. Reson. Med.* 1995; **34**: 343–352.
11. Mori S, van Zijl PCM. Diffusion weighting by the trace of the diffusion tensor within a single scan. *Magn. Reson. Med.* 1995; **33**: 41–52.
12. Ulug AM, van Zijl PCM. Orientation-independent diffusion imaging without tensor diagonalization: Anisotropy definitions based on physical attributes of the diffusion ellipsoid. *J. Magn. Reson. Imag.* 1999; **9**: 804–813.
13. Armitage PA, Bastin ME. Selecting an appropriate anisotropy index for displaying diffusion tensor imaging data with improved contrast and sensitivity. *Magn. Reson. Med.* 2000; **44**: 117–121.
14. Basser P, Jones DK. Diffusion-tensor MRI: Theory, experimental design, and data analysis. *NMR Biomed.* 2002; **15**: 456–467.
15. Conturo TE, McKinstry RC, Aronovitz JA, Neil JJ. Diffusion MRI: Precision, accuracy and flow effects. *NMR Biomed.* 1995; **8**: 307–332.
16. Mukherjee P, Miller JH, Shimony JS, Conturo TE, Lee BCP, Almli CR, McKinstry RC. Normal brain maturation during childhood: Developmental trends characterized with diffusion-tensor MR imaging. *Radiology* 2001; **221**: 349–358.
17. Morriss MC, Zimmerman RA, Bilaniuk LT, Hunter JV, Haselgrove JC. Changes in brain water diffusion during childhood. *Neuroradiology* 1999; **41**: 929–934.



18. Pierpaoli C, Jezzard P, Basser PJ, Barnett A, DiChiro G. Diffusion tensor MR imaging of the human brain. *Radiology* 1996; **201**: 637–648.
19. Shimony JS, McKinstry RC, Akbudak E, Aronovitz JA, Snyder AZ, Lori NF, Cull TS, Conturo TE. Quantitative diffusion-tensor anisotropy brain MR imaging: normative human data and anatomic analysis. *Radiology* 1999; **212**: 770–784.
20. Zacharopoulos NG, Narayana PA. Selective measurement of white matter and gray matter diffusion trace values in normal human brain. *Med. Phys.* 1998; **25**: 2237–2241.
21. Tanner SF, Ramenghi LA, Ridgway JP, Berry E, Saysell MA, Martinez D, Arthur RJ, Smith MA, Levene MI. Quantitative comparison of intrabrain diffusion in adults and preterm and term neonates and infants. *Am. J. Roentgenol.* 2000; **174**: 1643–1649.
22. Ulug AM, Beauchamp N Jr., Bryan RN, van Zijl PCM. Absolute quantitation of diffusion constants in human stroke. *Stroke* 1997; **28**: 483–490.
23. Dodge PR, Prenskey AL, Feigin RD. *Nutrition and the Developing Nervous System*. Mosby: St Louis, MO, 1975.
24. Klingberg T, Vaidya CJ, Gabrieli JD, Moseley ME, Hedehus M. Myelination and organization of the frontal white matter in children: a diffusion tensor MRI study. *Neuroreport* 1999; **10**: 2817–2821.
25. Neil JJ, McKinstry RC, Schlaggar BL, Schefft G, Shiran SI, Shimony JS, Snyder AZ, Almlí CR, Akbudak E, Conturo TE. Evaluation of diffusion anisotropy during human cortical grey matter development. *Proceedings of ISMRM, 8th Annual Meeting and Exhibition*, 2000; 591.
26. Neil JJ, McKinstry RC, Shiran SI, Snyder AZ, Conturo TE. Timing of changes on diffusion tensor imaging following brain injury in full-term infants. *Ann. Neurol.* 1998; **44**: 551.
27. Brody BA, Kinney HC, Kroman AS, Gilles FH. Sequence of central nervous system myelination in human infancy. I. An autopsy study of myelination. *J. Neuropathol. Exp. Neurol.* 1987; **46**: 283–301.
28. Beaulieu C. The basis of anisotropic water diffusion in the nervous system. *NMR Biomed.* 2002; **15**: 435–455.
29. Baratti C, Barnett AS, Pierpaoli C. Comparative MR imaging study of brain maturation in kittens with  $T_1$ ,  $T_2$ , and the trace of the diffusion tensor. *Radiology* 1999; **210**: 133–142.
30. Thornton JS, Ordidge RJ, Penrice J, Cady EB, Amess PN, Punwani S, Clemence M, Wyatt JS. Anisotropic water diffusion in white and gray matter of the neonatal piglet brain before and after transient hypoxia-ischaemia. *Magn. Reson. Imag.* 1997; **15**: 433–440.
31. Mori S, Itoh R, Zhang J, Kaufmann WE, van Zijl PC, Solaiyappan M, Yarowsky P. Diffusion tensor imaging of the developing mouse brain. *Magn. Reson. Med.* 2001; **46**: 18–23.
32. Marin-Padilla M. Ontogenesis of the pyramidal cell of the mammalian neocortex and developmental cytoarchitectonics: a unifying theory. *J. Comp. Neurol.* 1992; **321**: 223–240.
33. Mori S, van Zijl PCM. Fiber racking: Principles and strategies. *NMR Biomed.* 2002; **15**: 468–480.
34. Volpe JJ. *Neurology of the Newborn*. W.B. Saunders: Philadelphia, PA, 2001.
35. Taylor DL, Edwards AD, Mehmet H. Oxidative metabolism, apoptosis and perinatal brain injury. *Brain Pathol.* 1999; **9**: 93–117.
36. Seisjo BK, Wieloch T. Molecular mechanisms of ischemic brain damage:  $Ca^{2+}$ -related events. In: *Cerebrovascular Diseases*, Plum F, Pulsinelli W (eds). New York: Raven Press, 1999.
37. Buonocore G, Perrone S, Bracci R. Free radicals and brain damage in the newborn. *Biol. Neonate* 2001; **79**: 180–186.
38. Barks JD, Silverstein FS. Excitatory amino acids contribute to the pathogenesis of perinatal hypoxic-ischemic brain injury. *Brain Pathol.* 1992; **2**: 235–243.
39. Silverstein FS, Barks JD, Hagan P, Liu XH, Ivacko J, Szaflarski J. Cytokines and perinatal brain injury. *Neurochem. Int.* 1997; **30**: 375–383.
40. Nelson KB, Dambrosia JM, Grether JK, Phillips TM. Neonatal cytokines and coagulation factors in children with cerebral palsy. *Ann. Neurol.* 1998; **44**: 665–675.
41. Banker BQ, Larroche JC. Periventricular leukomalacia of infancy. *Arch. Neurol.* 1962; **7**: 386–410.
42. Huppi PS, Amato M. Advanced magnetic resonance imaging techniques in perinatal brain injury. *Biol. Neonate* 2001; **80**: 7–14.
43. Dammann O, Leviton A. Infection remote from the brain, neonatal white matter damage, and cerebral palsy in the preterm infant. *Semin. Pediatr. Neurol.* 1998; **5**: 190–201.
44. Perlman JM. White matter injury in the preterm infant: An important determination of abnormal neurodevelopment outcome. *Early Hum. Dev.* 1998; **53**: 99–120.
45. Zuckerman SL, Leffler CW, Shibata M. Recent advances and controversies in cerebrovascular physiology in the newborn. *Curr. Opin. Pediatr.* 1993; **5**: 162–169.
46. Greisen G, Vannucci RC. Is periventricular leukomalacia a result of hypoxic-ischaemic injury? Hypocapnia and the preterm brain. *Biol. Neonate* 2001; **79**: 194–200.
47. van Gelderen P, de Vleeschouwer MHM, DesPres D, Parker J, van Zijl PCM, Moonen CTW. Water diffusion and acute stroke. *Magn. Reson. Med.* 1994; **31**: 154–163.
48. Cowan FM, Pennock JM, Hanrahan JD, Manji KP, Edwards AD. Early detection of cerebral infarction and hypoxic ischemic encephalopathy in neonates using diffusion-weighted magnetic resonance imaging. *Neuropediatrics* 1994; **25**: 172–175.
49. Duong TQ, Ackerman JH, Ying HS, Neil JJ. Evaluation of extra- and intracellular apparent diffusion in normal and globally ischemic rat brain via  $^{19}\text{F}$  NMR. *Magn. Reson. Med.* 1998; **40**: 1–13.
50. Neil JJ, Duong TQ, Ackerman JH. Evaluation of intracellular diffusion in rat brain via  $^{133}\text{Cs}$  NMR. *Magn. Reson. Med.* 1996; **35**: 329–335.
51. Wick M, Nagatomo Y, Prielmeier F, Frahm J. Alteration of intracellular metabolite diffusion in rat brain *in vivo* during ischemia and reperfusion. *Stroke* 1995; **26**: 1930–1933.
52. van der Toorn A, Dijkhuizen RM, Tulleken CA, Nicolay K. Diffusion of metabolites in normal and ischemic rat brain measured by localized  $^1\text{H}$  MRS. *Magn. Reson. Med.* 1996; **36**: 914–922.
53. Ebisu T, Naruse S, Horikawa Y, Ueda S, Tanaka C, Uto M, Umeda M, Higuchi T. Discrimination between different types of white matter edema with diffusion-weighted MR imaging. *J. Magn. Reson. Imag.* 1993; **3**: 863–868.
54. Hinchey J, Chaves C, Appignani B, Breen J, Pao L, Wang A, Pessin MS, Lamy C, Mas JL, Caplan LR. A reversible posterior leukoencephalopathy syndrome. *New Engl. J. Med.* 1996; **334**: 494–500.
55. Ay H, Buonanno FS, Schaefer PW, Le DA, Wang B, Gonzalez RG, Koroshetz WJ. Posterior leukoencephalopathy without severe hypertension: utility of diffusion-weighted MRI. *Neurology* 1998; **51**: 1369–1376.
56. Mukherjee P, McKinstry RC. Reversible posterior leukoencephalopathy syndrome: evaluation with diffusion-tensor MR imaging. *Radiology* 2001; **219**: 756–765.
57. Braun KP, de Graaf RA, Vandertop WP, Gooskens RH, Tulleken KA, Nicolay K. *In vivo*  $^1\text{H}$  MR spectroscopic imaging and diffusion weighted MRI in experimental hydrocephalus. *Magn. Reson. Med.* 1998; **40**: 832–839.
58. Gideon P, Thomsen C, Gjerris F, Sorensen PS, Henriksen O. Increased self-diffusion of brain water in hydrocephalus measured by MR imaging. *Acta Radiol.* 1994; **35**: 514–519.
59. Hüppi P, Murphy B, Maier S, Inder T, Zientara G, Jolesz F, Volpe J. Diffusion tensor imaging in neonatal post hemorrhagic hydrocephalus. *Proceedings of ISMRM, 9th Annual Meeting and Exhibition*, 2001; 1556.
60. Welch KMA, Windham J, Knight RA, Nagesh V, Hugg JW, Jacobs M, Peck D, Booker P, Dereski MO, Levine SR. A model to predict the histopathology of human stroke using diffusion and  $T_2$ -weighted magnetic resonance imaging. *Stroke* 1995; **26**: 1983–1989.
61. Li F, Han SS, Tatlisumak T, Liu KF, Garcia JH, Sotak CH, Fisher M. Reversal of acute apparent diffusion coefficient abnormalities and delayed neuronal death following transient focal cerebral ischemia in rats. *Ann. Neurol.* 1999; **46**: 333–342.
62. Copen W, Schwamm L, Gonzalez R, Wu O, Harmath C, Schaefer P, Koroshetz W, Sorensen A. Ischemic stroke: effects of etiology and patient age on the time course of the core apparent diffusion coefficient. *Radiology* 2001; **221**: 27–34.
63. Forbes KP, Pipe JG, Bird R. Neonatal hypoxic-ischemic encephalopathy: Detection with diffusion-weighted MR imaging. *Am. J. Neuroradiol.* 2000; **21**: 1490–1496.

64. Inder T, Huppi PS, Zientara GP, Maier SE, Jolesz FA, di Salvo D, Robertson R, Barnes PD, Volpe JJ. Early detection of periventricular leukomalacia by diffusion-weighted magnetic resonance imaging techniques. *J. Pediatr.* 1999; **134**: 631–634.
65. Wolf RL, Zimmerman RA, Clancy R, Haselgrove JH. Quantitative apparent diffusion coefficient measurements in term neonates for early detection of hypoxic-ischemic brain injury: Initial experience. *Radiology* 2001; **218**: 825–833.
66. Lin SP, Song SK, Miller JP, Ackerman JJ, Neil JJ. Direct, longitudinal comparison of (1)H and (23)Na MRI after transient focal cerebral ischemia. *Stroke* 2001; **32**: 925–932.
67. Wang PY, Barker PB, Wityk RJ, Ulug AM, van Zijl PCM, Beauchamp NJ Jr., Diffusion-negative stroke: A report of two cases. *Am. J. Neuroradiol.* 1999; **20**: 1876–1880.
68. Barkovich AJ, Westmark K, Partridge C, Sola A, Ferriero DM. Perinatal asphyxia: MR findings in the first 10 days. *Am. J. Neuroradiol.* 1995; **16**: 427–438.
69. Rutherford MA, Cowan FM, Manzur AY, Dubowitz LMS, Pennock JM, Hajnal JV, Young IR, Bydder GM. MR imaging of anisotropically restricted diffusion in the brain of neonates and infants. *J. Comput. Assist. Tomogr.* 1991; **15**: 188–198.
70. Klingberg T, Hedehus M, Temple E, Salz T, Gabrieli JD, Moseley ME, Poldrack RA. Microstructure of temporo-parietal white matter as a basis for reading ability: evidence from diffusion tensor magnetic resonance imaging. *Neuron* 2000; **25**: 493–500.
71. Pierpaoli C, Barnett A, Pajevic S, Chen R, Penix LR, Virta A, Basser P. Water diffusion changes in wallerian degeneration and their dependence on white matter architecture. *Neuroimage* 2001; **13**: 1174–1185.
72. Volpe JJ. Brain injury in the premature infant—current concepts. *Prev. Med.* 1994; **23**: 638–645.
73. Huppi PS, Murphy B, Maier SE, Zientara GP, Inder TE, Barnes PD, Kikinis R, Jolesz FA, Volpe JJ. Microstructural brain development after perinatal cerebral white matter injury assessed by diffusion tensor magnetic resonance imaging. *Pediatrics* 2001; **107**: 455–460.